*Pollution, 5(2): 257-268, Spring 2019*
DOI: 10.22059/poll.2018.260252.463
Print ISSN: 2383-451X Online ISSN: 2383-4501
Web Page: https://jpoll.ut.ac.ir, Email: jpoll@ut.ac.ir

# Monitoring of SO2 Column Concentration Over Iran Using Satellite-based Observations during 2005-2016

**Salmabadi, H. and Saeedi, M.***

Environmental Research Laboratory, School of Civil Engineering, Iran University of Science and Technology, Narmak, Tehran 16846, Iran

Received: 04.10.2018 Accepted: 21.12.2018

**ABSTRACT:** For the first time, sulfur dioxide concentration was monitored between 2005 and 2016 over Iran which is among the countries with a high $SO_2$ emission rate in the world. To that end, $SO_2$ column concentration at Planetary Boundary Layer (PBL) from Ozone Monitoring Instrument (OMI) was analyzed. OMI is a sensor onboard the Aura satellite which can measure daily $SO_2$ concentration on the global scale. From OMI maps, 19 notable $SO_2$ hotspots were detected over Iran. The results indicate that the most elevated level of $SO_2$ among these 19 hotspots belong to Khark Island and Asaluye in Bushehr province, southwest of Iran. Annual trend analysis shows that $SO_2$ concentration has been slightly augmented during 2005-2016 over this country. Distribution analysis of $SO_2$ concentration over Iran showed that the most polluted provinces are Bushehr, Khuzestan and Ilam lied in the southwest of Iran. On the contrary, the lowest level of $SO_2$ has observed over northwest of Iran at West and East Azerbaijan and Ardabil provinces. The correlation coefficient between total energy production in Iran and $SO_2$ concentration from 2005 to 2016 is as high as ~0.7. Hence, it can be derived that energy production, most notably production of crude oil, plays a pivotal role in $SO_2$ concentration over Iran.

**Keywords:** Sulfur Dioxide, Iran, Aura, OMI, Trace Gases, GIS.

## INTRODUCTION

Sulfur dioxide ($SO_2$) is a conventional pollutant whose measurement is vital to air quality assessment (Nikolić et al., 2010). Direct exposure to sulfur dioxide is lethal for human health and may cause respiratory illnesses (Afif et al., 2008; Fioletov et al., 2013; Klimont et al., 2013; Smith et al., 2011). Through chemical reaction in the atmosphere, it forms sulfate aerosols and sulfuric acid which can harm human and ecosystem directly and indirectly (Fioletov et al., 2015; Fioletov et al., 2013; Lu et al., 2013). The lifetime of sulfate aerosols in the atmosphere is longer than sulfur dioxide (Krotkov et al., 2006; Wang et al., 2013), therefore, it has a strong ability to prompt climate change through upsetting energy equilibrium of the earth system and changing the cloud formation mechanism (Fioletov et al., 2013; Jiang et al., 2012; Krotkov et al., 2015a). Moreover, sulfuric acid leads to acid rain which threatens biosphere, and acidify water and soil (Krotkov et al., 2015a; Smith et al., 2011). Sulfur dioxide liberates into the atmosphere through natural and anthropogenic sources (Lu et al., 2013). Oil and gas industries, power plants, and smelters are considered as the most marked anthropogenic sources (Fioletov et al., 2015; Fioletov and McLinden, 2016) while volcanic eruption

* Correspondence author, Email: msaeedi@iust.ac.ir

is the main natural one (Beirle et al., 2014; Fioletov and McLinden, 2016).

Atmospheric pollution monitoring has been done conventionally via surface base observations which are relatively precise, but their spatial and temporal coverage is constrained (Jiang et al., 2012). Hence, measurement and trend analysis of atmospheric pollutants are implausible through this kind of monitoring technique. Remote sensing methods provide a broad spatial coverage with a wide temporal range which makes it possible to evaluate the variation of the atmospheric pollutants throughout the history. Therefore, a lot of studies have been conducted using remote sensing technique for monitoring of $SO_2$ (Fioletov et al., 2015; Fioletov et al., 2013; Fioletov et al., 2016; Jiang et al., 2012; Krotkov et al., 2015a; Krotkov et al., 2010; Lu et al., 2013). There is a wide assortment of satellites that carry a sensor for monitoring and measurement of $SO_2$ concentration in the atmosphere. Table 1 demonstrates these satellites and their sensors with the corresponding lunch date. Among which, Ozone Monitoring Instrument (OMI) has the finest spatial resolution (13 * 24 km2 at nadir) (Fioletov et al., 2011) and is expedient for detecting sulfur dioxide in the lower atmosphere (Jiang et al., 2012). Fine horizontal resolution alongside its daily temporal resolution made this sensor suitable for long-term monitoring purposes.

Based on JRC/PBL (2011) projection Iran liberated ~1370 kton sulfur dioxide into the atmosphere in 2010 and is the most sulfur dioxide producing country in the world after China, USA, India, Saudi Arabia, Russia, South Africa, Indonesia, Kazakhstan, and Turkey with emission rate of 30000, 10100, 95000, 2800, 2600, 2300, 2000, 1600, 1500, 1400 kton/year, respectively. In a recent study conducted by Fioletov et al. (2016) the emission rate of sulfur dioxide from 491 notable sources all around the world was estimated using satellite-based data. Accordingly, about 1500 kton of $SO_2$ was produced from 15 major sources in Iran in 2014. $SO_2$ pollution over Iran was previously reported by Fioletov et al. (2013) and Krotkov et al. (2015a). Although this country is a consequential producer of sulfur dioxide in the world, to the author's knowledge, no study has been monitored this gaseous pollution over this country. Therefore, the main focus of this research is the analysis of $SO_2$ concentration fluctuation over Iran between 2005 and 2016 using satellite-based observations. Furthermore, major sources of $SO_2$ in this country and the most polluted provinces will be determined.

**Table 1. Remote sensing instruments for sulfur dioxide monitoring (Campion et al., 2010; Carboni et al., 2012; Eleftheriadis et al., 2006; Fioletov et al., 2013; Henney et al., 2012; Jiang et al., 2012; Theys et al., 2013)**

| Satellite | Sensor | Launch date | Satellite | Sensor | Launch date |
|---|---|---|---|---|---|
| Nimbus-7 | Total Ozone Mapping Spectrometer(TOMS) | 1978 | Aqua | Atmospheric Infrared Sounder(AIRS) | 2002 |
| European Remote-Sensing Satellite (ERS-2) | Global Ozone Monitoring Experiment(GOME) | 1995 | Meteosat Second Generation (MSG) | Spinning Enhanced Visible and Infrared Imager (SEVIRI) | 2002 |
| Earth Probe | Total Ozone Mapping Spectrometer(TOMS) | 1996 | Aqua | MODIS | 2002 |
| Terra | MODIS | 1999 | Aura | Microwave Limb Sounder(MLS) | 2004 |
| Terra | Advanced Spaceborne Thermal Emission and Reflection Radiometer (ASTER) | 1999 | Aura | Ozone Monitoring Instrument(OMI) | 2004 |
| Environmental Satellite-1 (ENVISAT-1) | SCanning Imaging Absorption spectroMeter for Atmospheric CHartographY (SCIAMACHY) | 2002 | MetOp-A | IASI | 2007 |

## MATERIAL AND METHODS

Aura is a sun-synchronized satellite which started to work in July 2004 (Lu et al., 2013; Parkinson et al., 2006). Ozone monitoring instrument (OMI) is the most important sensor among Aura's four sensors, and it is designed to continue Backscatter UltraViolet (BUV) sensor of Nimbus-4 (Parkinson et al., 2006). OMI can measure daily $NO_2$, $SO_2$, $O_3$, and aerosols on the global scale (Lu et al., 2013). OMI records data in ultraviolet-visible range (270-600 nm) with a view angle of 114 and spatial resolution of 24 km*13 km at nadir to about 28 km*150 km at outermost swath angle (Fioletov et al., 2015; Jiang et al., 2012; Lu et al., 2013). In this study, level-3 $SO_2$ data has been collected from GIOVANNI (Geospatial Interacvtive Online Visualization And aNalysis Infrastracture) online software (Krotkov et al., 2015b). This online software has been developed by The National Aeronautics and Space Administration (NASA) Goddard Earth Science Data and Information Services Center (GES DISC) and is accessible at (http://disc.sci.gsfc.nasa.gov/giovanni).

Level-3 $SO_2$ data contain column concentration in the planetary boundary layer (PBL) and are produced with Band Residual Difference (BRD) algorithm which is sensitive to anthropogenic emissions (Fioletov et al., 2015; Krotkov et al., 2015b). The spatial resolution of level-3 data is 0.25*0.25 degree (1 degree~ 100km) and available since October 2004. $SO_2$ in the PBL layer mostly correspond to anthropogenic sources (Jiang et al., 2012) while $SO_2$ from volcanic eruptions discharges to the levels out of PBL layer (Fioletov et al., 2015). Therefore, level-3 $SO_2$ data is expedient for monitoring the concentration variation over Iran which has many anthropogenic sources. OMI data had widely been used in many studies to monitoring $SO_2$ concentration regionally and globally (Fioletov et al., 2015; Fioletov et al., 2011; Fioletov et al., 2013; Fioletov et al., 2016; Jiang et al., 2012; Krotkov et al., 2015a; Lu et al., 2013). In this study, level-3 PBL $SO_2$ data were acquired from GIOVANNI between 1 January 2005 and 31 December 2016, seasonally. For further processing, these data were exported to a GIS software. Firstly, from seasonal data, mean $SO_2$ concentration was calculated for whole study period 2005-2016 (Overall mean concentration) to derive distribution map of $SO_2$ concentration and to determine the most polluted regions (Hotspots of sulfur dioxide) of Iran. Secondly, the mean concentration of $SO_2$ was calculated for each year between 2005 and 2016 (Annual mean concentration) to analyze the annual trend of $SO_2$ level over the entire country. Thirdly, from seasonal data, mean $SO_2$ concentration level was also computed for the whole study period seasonally to track the changes in $SO_2$ concentration from season to season over Iran. The flowchart in figure 1 presents an overview of the complete methodology.

## RESULTS AND DISCUSSION

Figure 2 shows the mean level of $SO_2$ for the period between January 2005 and December 2016 and depicts the major hotspots of sulfur dioxide over Iran. As it is evident in figure 2, there are 19 notable hotspots which are distributed unevenly over this country. The location of these hotspots, which most of them were introduced as major emission origins in the previous studies (Fioletov et al., 2013; Fioletov et al., 2016; Krotkov et al., 2015a), is determined in Figure 2.

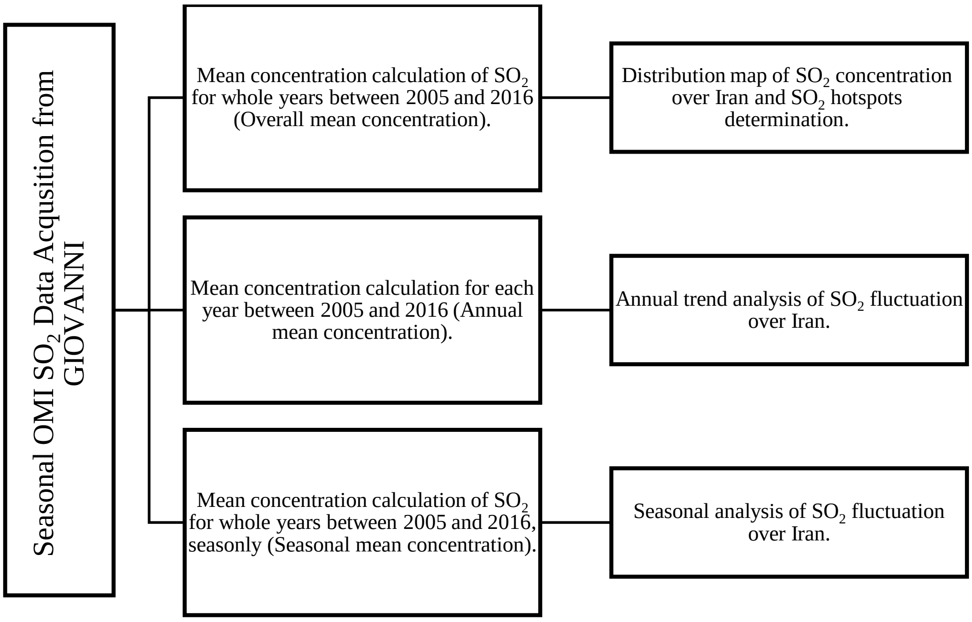


**Fig. 1. Methodology flowchart**

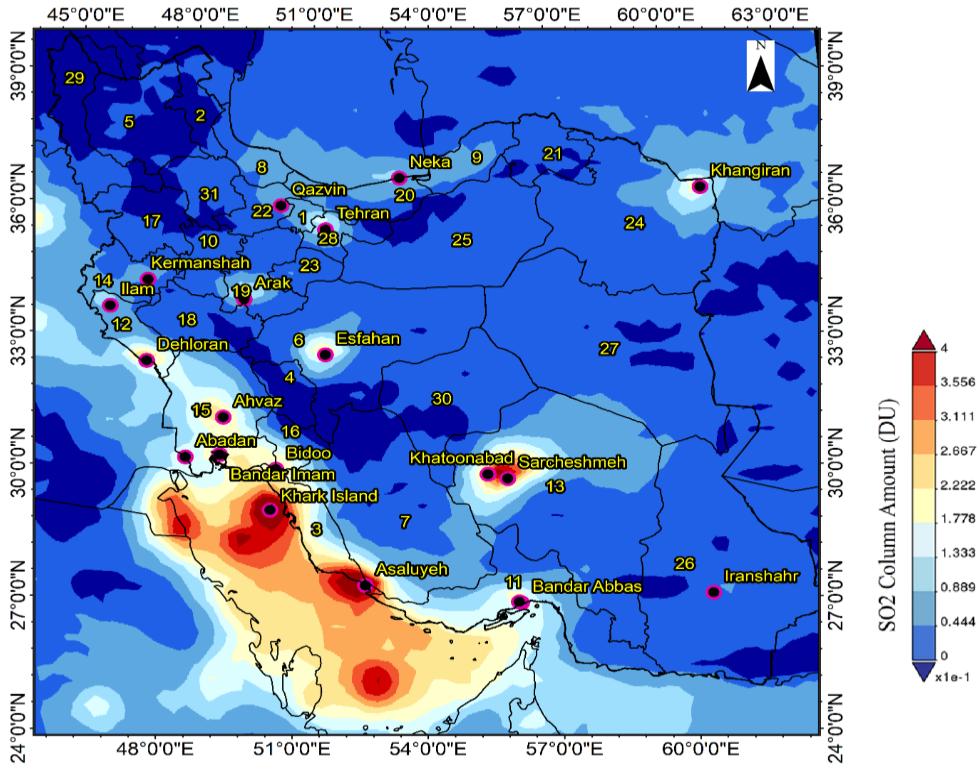


**Fig. 2. Distribution of the average PBL $SO_2$ column concentration over Iran. The average was taken for the period from January 2005 to December 2016. The location of the enhanced level of $SO_2$ is determined as pink dots. Each province is shown with a number: 1, Alborz; 2, Ardabil; 3, Bushehr; 4, Chaharmahal and Bakhtiari; 5, East Azerbaijan; 6, Esfahan; 7, Fars; 8, Gilan; 9, Golestan; 10, Hamedan; 11, Hormozgan; 12, Ilam; 13, Kerman; 14, Kermanshah; 15, Khuzestan; 16, Kohgiluyeh and Boyer Ahmad; 17, Kurdistan; 18, Lorestan; 19, Markazi; 20, Mazandaran; 21, North Khorasan; 22, Qazvin; 23, Qom; 24, Razavi Khorasan; 25, Semnan; 26, Sistan and Baluchistan; 27, South Khorasan; 28, Tehran; 29, West Azerbaijan; 30, Yazd; 31, Zanjan.**

To further investigation, the inter-annual analysis of $SO_2$ level over Iran's hotspots during 2005-2016 was also conducted (Figure 3). To this end, the summation of the $SO_2$ values (Total $SO_2$ from now on) were calculated for all the pixels around each of the emission sources within a radius of 60 km since the current OMI sensor detects the elevated $SO_2$ values within a radius of ~60 km around a source (Lu et al., 2013).

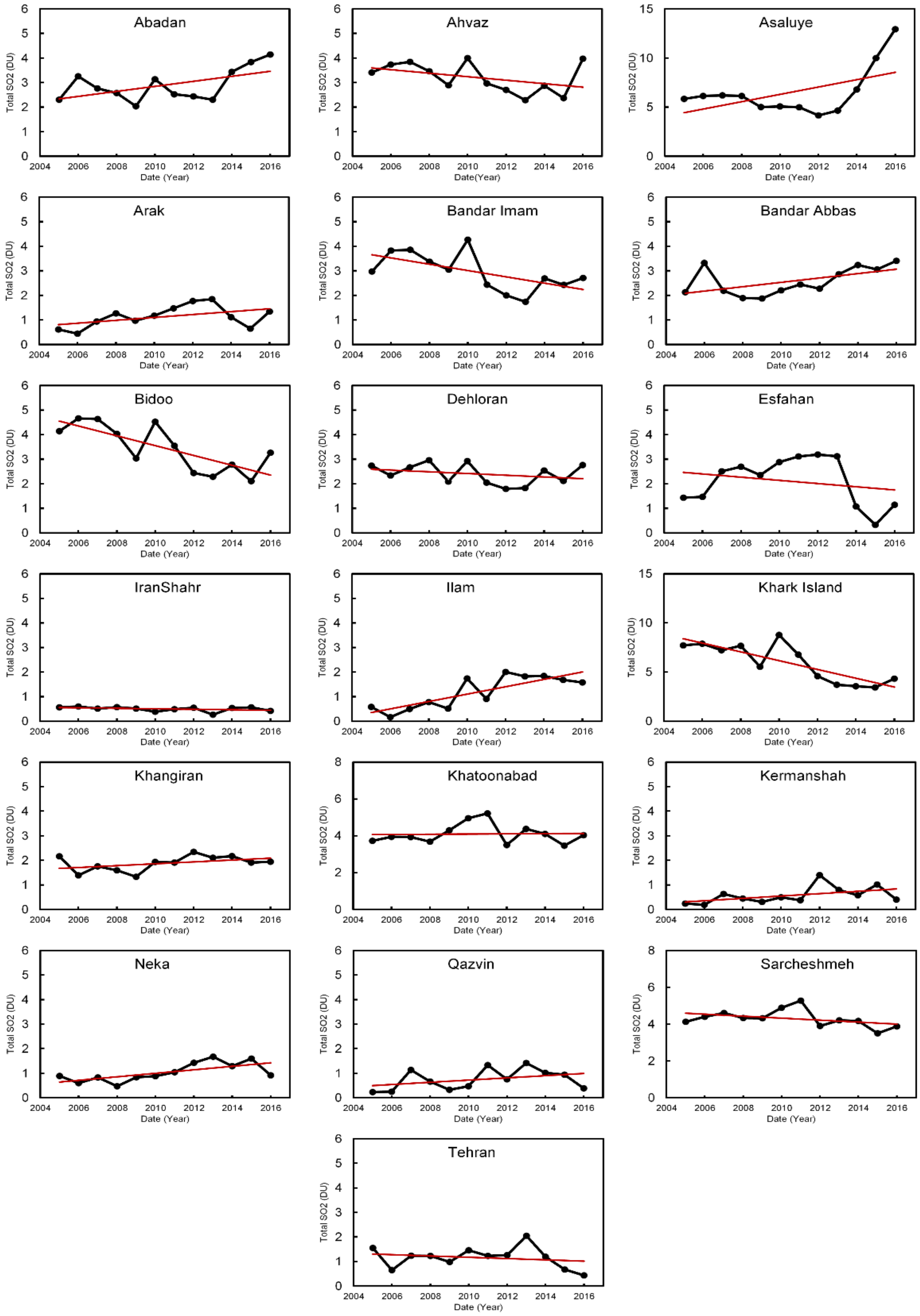


**Fig. 3. Variation of the yearly sum of OMI $SO_2$ concentration over Iran's hotspots between 2005 and 2016. Note the discerepensy in the Y-axis scales of Asaluye, Khark Island, Sarcheshmeh and Khatoonabad panels. The location of the hotspots is defined in figure 2.**

As it was mentioned before, based on figure 2, the distribution of $SO_2$ column concentration over Iran is spatially imbalanced. The majority of the hotspots are located in the southwest of this country and the Persian Gulf where many oil and gas industries operate. The highest concentration of $SO_2$ is observed over Khark Island (Mean total $SO_2$ of ~6 DU between 2005 and 2016) and Asaluye (Mean total $SO_2$ of ~6.5 DU between 2005 and 2016) in Bushehr province which primarily associated with oil and gas industries (Including Kharg Petrochemical Company in Khark Island and South Pars Gas Complex in Asaluye). Based on the inter-annual analysis of total $SO_2$ around these sources (Figure 3) Khark Island's emission significantly reduced by 42% from 2005 to 2016 while the total $SO_2$ around the Asaluye sharply increased by 120% from 2005 to 2016. 8 new phases of South Pars Gas Complex was exploited between 2008 and 2013 (S.P.G.C, 2018). This can be potentially attributed to the significant increment in $SO_2$ level over Asaluye. As the OMI measurements show (Figure 4), the $SO_2$ level around Khark Island and Asaluye varied conspicuously from 2005 to 2016.

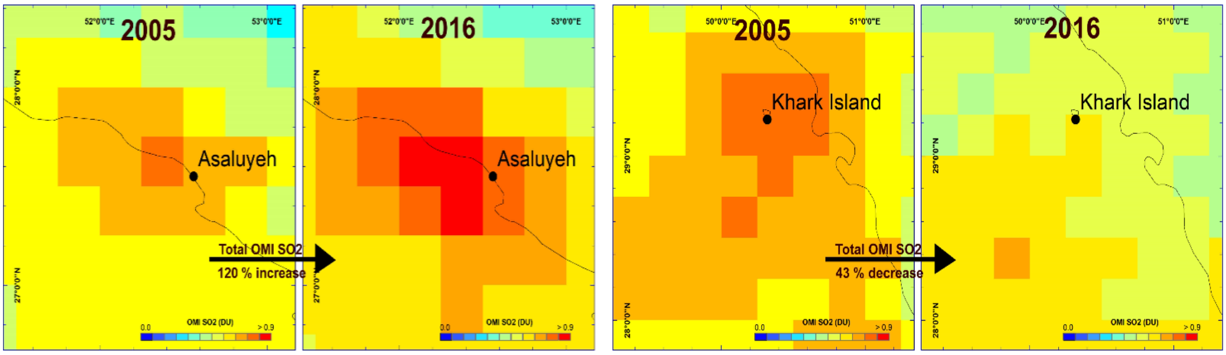


**Fig. 4. OMI $SO_2$ level around Asaluye and Khark Island in 2005 and 2016.**

Khuzestan is another province which is drastically affected by high levels of $SO_2$ in Iran. Ramin Power Plant, Marun Petrochemical Company, and Khuzestan Steel Company in Ahvaz along with Bandar Imam Petrochemical Company in Bandar Imam, Abadan Refinery, and oil wells are the main $SO_2$ origins in this Province. The inter-annual analysis shows that the total OMI $SO_2$ concentration around Ahvaz and Bandar Imam slightly decreased while the total concentration of Abadan's hotspot exhibited a sign of increase. Bandar Abbas Oil Refining Company and Bandar Abbas Thermal Power Plant make Hormozgan province as one the most polluted regions in Iran. The total $SO_2$ concentration over Bandar Abbas's hotspot increased by 59 % from 2005 to 2016. Production increase in Bandar Abbas Oil Refining Company in 2008 and 2012 (B.O.R.C, 2018) and exploit of a new refinery named Persian Gulf Star Oil Company (P.G.S.O.C) in recent years may give rise to the increment of $SO_2$ concentration in this province. Dehloran oil fields, Ilam Gas Treating and Kermanshah Oil Refining Company make the main there hotspots of sulfur dioxide in western Iran. Based on the inter-annual analysis, although the intensity of the hotspots over Ilam Gas Treating and Kermanshah Oil Refining Company is not significant compared with the other Iran's refineries, an increasing trend in $SO_2$ concentration over them is notable. As it is evident in figure 2, another significantly enhanced level of $SO_2$ is readily observable over Kerman province which is related to two copper smelters (Khatoonabad and Sarcheshmeh Copper Smelters) in this region (Salmabadi & Saeedi, 2018). The mean of total $SO_2$ concentration for the study period (2005-2016) over Khatoonabad and Sarcheshmeh Copper Smelters are ~4 DU and ~4.3 DU, respectively. In spite of the high intensity of atmospheric pollution over this region, trend analysis indicates that the total concentration of this $SO_2$ enhanced level has not changed much during the study period (Figure 3). For example, the $SO_2$ emission rate of Sarcehshmeh Copper Smelter in 2005 and 2014 was 253 kt/year and 227 kt/year, respectively (Fioletov et al., 2016). Another distinct and notable $SO_2$ enhanced level is apparent northeast of Iran related to Shahid Hashemi Nejad (Khangiran) Gas Processing Company near Sarakhs in Razavi Khorasan. Based on the inter-annual analysis, total $SO_2$ level over Khangiran Gas Processing Company remained approximately unchanged (~1.9 DU) during 2005-2016. Two noticeable sulfur dioxide hotspots over two megacities of Iran including Esfahan, and Tehran are also discernible. Two steel smelters (Mobarakeh Steel Company and Esfahan Steel Company), Sepahan Oil Company, Islamabad Power Plant and even transportation activity give rise to the enhanced level of $SO_2$ in Esfahan. Inter-annual analysis of total OMI $SO_2$ over Esfans's hotspot indicates an abrupt decrease between 2013 and 2014. It was previously reported that the emission rate of Sepahan Oil Company reduced by ~63% from 2013 to 2014 (Fioletov et al., 2016). This could be potentially attributed to the mentioned sudden decrease in $SO_2$ concentration of Esfahan's hotspot. Power plants, Tehran Oil Refining Company, and transportation activity are mainly responsible for $SO_2$ emission in Tehran. The inter-annual analysis shows that the total $SO_2$ concentration over Tehran has not significantly changed during the study period (Figure 3). Some other hotspots are also detectable over Arak, Qazvin, Iranshahr and Neka cities. The primary emission sources in the mentioned cities are Shazand (Arak) Thermal Power Plant and Imam Khomeini Oil Refining Company near Arak, Shahid Rajaee Thermal Power Plant near Qazvin, Bampour Power Plant in Iranshahr and Shahid Salimi Power Plant near Neka. The inter-annual analysis of these enhanced level is shown in Figure 3.

There is a significant discrepancy in the average concentration of OMI $SO_2$ among the 31 provinces of Iran (Figure 5). The most polluted provinces are located southwest of Iran. Bushehr has the highest mean concentration level of sulfur dioxide, followed by Khuzestan, Ilam, Hormozgan, Kerman, Alborz, and Tehran (Figure 5). On the other hand, West Azerbaijan, Chaharmahal and Bakhtiari, East Azerbaijan, North Khorasan, Kurdistan, and Ardabil have the lowest concentration of $SO_2$ among all provinces (Figure 5).

Based on Figure 5, Kermanshah, which was not among the profoundly affected provinces during 2005-2007, confronted a continuous increment in $SO_2$ concentration during 2008-2016. Ilam and Hormozgan also exhibited a sign of increase between 2005 and 2016 (Figure 5). Northern provinces of Iran including Gilan, Golestan, and Mazandaran are also among areas whose $SO_2$ concentration have increased during the study period. The significant increment (416% from 2005 to 2014) in $SO_2$ emission rate of Neka Power Plant probably contribute to the growing trend in $SO_2$ concentration over Gilan, Golestan, and Mazandaran provinces. On the other hand, based on figure 5, a decreasing trend of $SO_2$ concentration during 2005-2016 observed over Kohgiluyeh and Boyer Ahmad. The $SO_2$ level over Khuzestan, and Bushehr provinces, which are among areas with the high level of $SO_2$, also reduced between 2005 and 2013, but an increase in sulfur dioxide level can be notified between 2014 and 2016. Other provinces exhibited a sign of growth or approximately a consistency in OMI $SO_2$ concentration during the study periods. This may highlight further needs for some control management strategies by the authorities.

The seasonal analysis of variation of mean total OMI $SO_2$ concentration over Iran shows that the $SO_2$ level is maximum in autumn and winter while it is minimum in spring and summer (Figure 6). Power plants mainly use Mazut instead of natural gas in colder seasons, and also PBL depth in autumn and winter is much less than summer and spring (Leelőssy et al., 2014) which culminates in a high $SO_2$ concentration in autumn and winter over Iran.

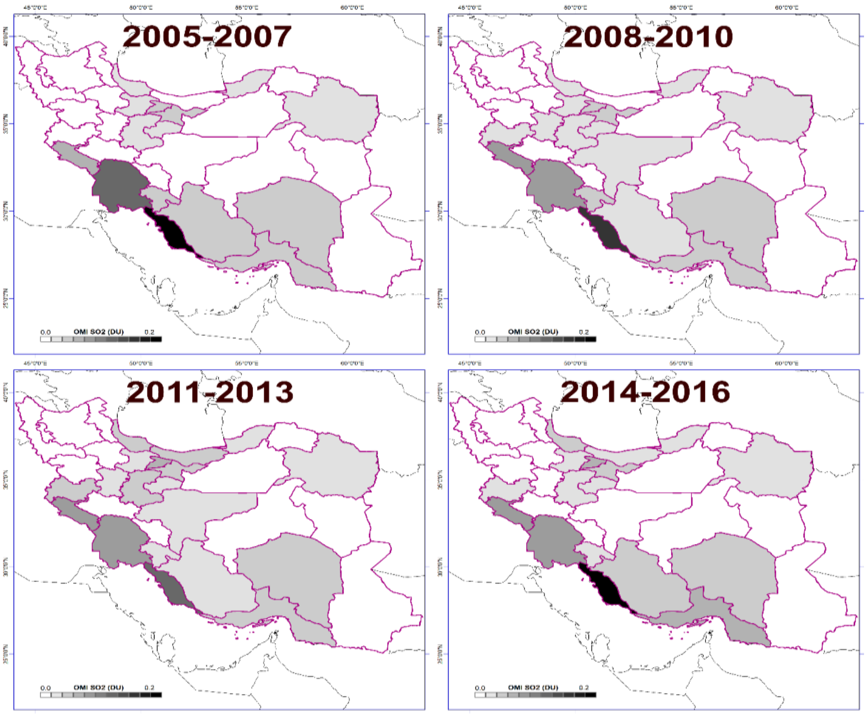


**Fig. 5. The average of OMI $SO_2$ concentration for 31 provinces of Iran (provinces as defined in figure 2). The averages of OMI $SO_2$ concentration were taken for four different periods: 2005-2007, 2008-2010, 2011-2013, and 2014-2016.**

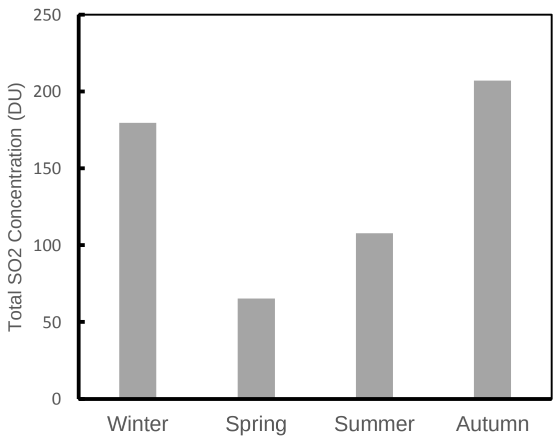


**Fig. 6. Seasonal variability of total $SO_2$ column concentration over entire Iran. Seasonal averages were taken for the period from January 2005 to December 2016.**

The annual fluctuation analysis of total $SO_2$ concentration over Iran shows an oscillation between 2005 and 2012, and after 2012 the $SO_2$ level over Iran has slightly increased (Figure 7). The maximum total column concentration of $SO_2$ during the study period occurred in 2010 and 2016, and the minimum total $SO_2$ level was in 2006 and 2012. The fluctuation of total energy (Including oil, gas, electricity, coal, biomass, and heat) production and total energy consumption over Iran between 2005 and 2016 is also depicted in Figure 7 (Enerdata, 2018). The correlation coefficient between fluctuation of total energy production in Iran and total OMI $SO_2$ concentration is ~0.70, and the correlation coefficient between the variation of total energy consumption in Iran and total OMI $SO_2$ concentration is only ~0.05. Consequently, to a certain degree, the $SO_2$ level over Iran is highly correlated with energy production.

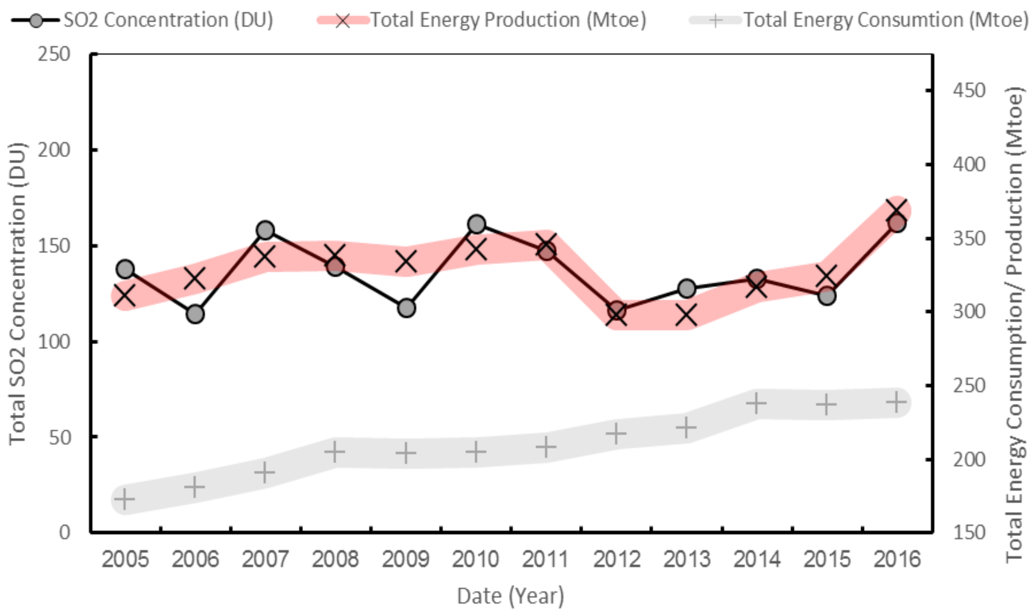


**Fig. 7. Variations in annual total OMI $SO_2$ concentration (DU) coupled with the yearly fluctuation of total energy consumption/production (million tons of oil equivalent (Mtoe)) in Iran from 2005 to 2016**

Since the production of crude oil is the primary form of energy production in Iran, annual changes in total $SO_2$ concentration and crude oil production from 2005 to 2016 was investigated (OPEC, 2017; OPEC, 2013; OPEC, 2009; OPEC, 2005) (Figure 8). As it is evident in figure 8, there is an abrupt reduction in both the total $SO_2$ concentration and crude oil production from 2011 to 2012 (Red dashed circle in figure8). The USA tightened its sanction on Iran's oil in 2012 which made a considerable obstacle for Iran's oil trading. Consequently, crude oil production in Iran sharply decreases by %18 from 2011 to 2012 (OPEC, 2013) which cause a decrease in total $SO_2$ concentration over Iran in that year. A significant increment is occurred in total $SO_2$ level over Iran from 2015 to 2016 as the crude oil production increased by 24% (OPEC, 2017) (Blue dashed circle in figure 8). This support the high correlation between total energy production, most notably crude oil production, and the $SO_2$ concentration over Iran.

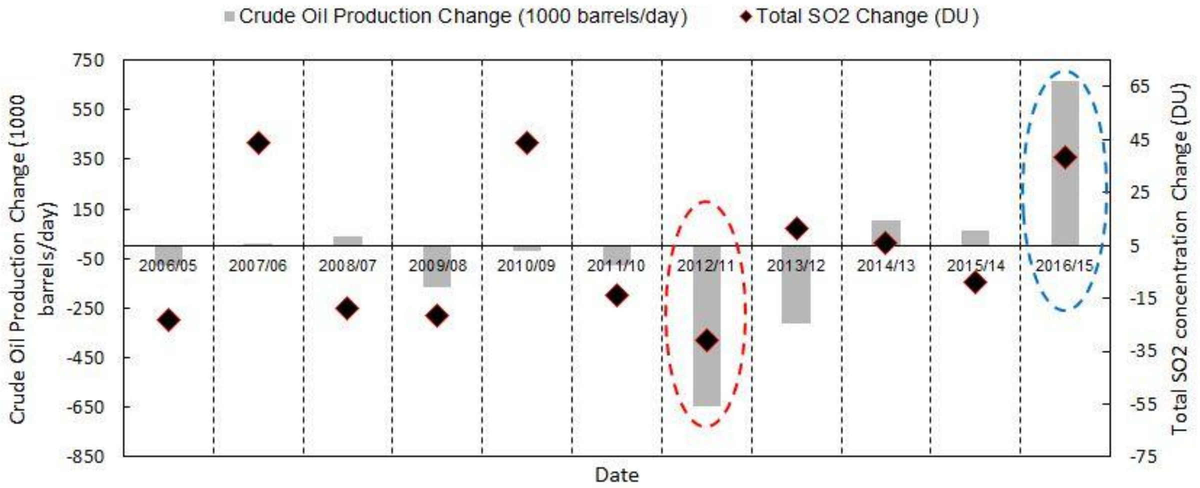


**Fig. 8. Annual changes in total $SO_2$ concentration and crude oil production in Iran from 2005 to 2016.**

## CONCLUSION

This study has investigated for the first time the $SO_2$ concentration level over Iran during 2005-2016 using PBL $SO_2$ column concentration data which was acquired from OMI sensor. Distribution map of $SO_2$ concentration over Iran shows that the spatial distribution of sulfur dioxide over this country is uneven. A significant bulk of $SO_2$ is detectable over the Persian Gulf and provinces lied in the southwest of Iran. Accordingly, the highest concentration of $SO_2$ observed over Khark Island and Asaluye. Total $SO_2$ concentration over Khark Island significantly reduced by 42% from 2005 (~7.7 DU) to 2016 (~4.3 DU) while the total $SO_2$ concentration of Asaluye's hotspot sharply augmented by 120% from 2005 (~5.8 DU) to 2016 (~12.93 DU). The results obtained from the annual analysis showed that the concentration of $SO_2$ over Iran between 2005 and 2016 had increased slightly and most of Iran's provinces exhibited a sign of growth during the study period. Bushehr, Khuzestan, Ilam, Hormozgan, Kerman, Alborz and Tehran are the most polluted provinces, respectively. On the other hand, West Azerbaijan, Ardabil, Chaharmahal and Bakhtiari, East Azarbaijan, North Khorasan and Kurdistan had lowest levels of $SO_2$ during 2005-2016. The analysis of changes mechanism of $SO_2$ concentration over Iran showed that there is a notable correlation between total energy production and $SO_2$ concentration during the study period. This highlights the significant role of energy production, specially crude oil production, on $SO_2$ pollution over Iran. Hence, the key to accomplishing the emission reduction target over Iran is to curb the emissions from energy production units. Therefore, there is much toil to be done to bring down $SO_2$ concentration across Iran. The present study examined the regional and temporal fluctuation of $SO_2$ level which provides better insight into the environmental situation in Iran and may help authorities to take more efficient management strategies.

## ACKNOWLEDGMENTS

The authors are grateful of Atmospheric Research Center of Iran University of Science and Technology for its support of this research. We also would like to thank GIOVANNI (Geospatial Interacvtive Online Visualization And aNalysis Infrastracture) online software maintaining by The National Aeronautics and Space Administration (NASA) Goddard Earth Science Data and Information Services Center (GES DISC) for providing OMI SO2 data.

## REFERENCES

Afif, C., Chélala, C., Borbon, A., Abboud, M., Adjizian-Gérard, J., Farah, W., Jambert, C., Zaarour, R., Saliba, N.B. and Perros, P.E. (2008). SO2 in Beirut: air quality implication and effects of local emissions and long-range transport. Air Qual. Atmos. Hlth., 1, 167-178.

Beirle, S., Hörmann, C., Penning de Vries, M., Dörner, S., Kern, C. and Wagner, T. (2014). Estimating the volcanic emission rate and atmospheric lifetime of SO 2 from space: a case study for Kīlauea volcano, Hawaii. Atmos. Chem. Phys., 14, 8309-8322.

B.O.R.C. (2018). Introduction of Bandar Abbas Oil Refining Company. Retrieved August, 2018, from http://www.baorco.ir/.

Campion, R., Salerno, G.G., Coheur, P.-F., Hurtmans, D., Clarisse, L., Kazahaya, K., Burton, M., Caltabiano, T., Clerbaux, C. and Bernard, A. (2010). Measuring volcanic degassing of SO 2 in the lower troposphere with ASTER band ratios. J. Volcanol. Geoth. Res., 194, 42-54.

Carboni, E., Grainger, R., Walker, J., Dudhia, A. and Siddans, R. (2012). A new scheme for sulphur dioxide retrieval from IASI measurements: application to the Eyjafjallajökull eruption of April and May 2010. Atmos. Chem. Phys., 12, 11417-11434.

Eleftheriadis, K., Colbeck, I., Housiadas, C., Lazaridis, M., Mihalopoulos, N., Mitsakou, C., Smolik, J. and Ždímal, V. (2006). Size distribution, composition and origin of the submicron aerosol in the marine boundary layer during the eastern Mediterranean "SUB-AERO" experiment. Atmos. Environ., 40, 6245-6260.

ENERDATA, Y. (2018). Global Energy Statistical Yearbook 2018. Retrieved August, 2018, from https://www.enerdata.net.

Fioletov, V., McLinden, C., Krotkov, N. and Li, C. (2015). Lifetimes and emissions of SO2 from point sources estimated from OMI. Geophys. Res. Lett., 42, 1969-1976.

Fioletov, V., McLinden, C., Krotkov, N., Moran, M. and Yang, K. (2011). Estimation of SO2 emissions using OMI retrievals. Geophys. Res. Lett., 38, L21811.

Fioletov, V., McLinden, C., Krotkov, N., Yang, K., Loyola, D., Valks, P., Theys, N., Van Roozendael, M., Nowlan, C. and Chance, K. (2013). Application of OMI, SCIAMACHY, and GOME-2 satellite SO2 retrievals for detection of large emission sources. J. Geophys. Res. Atmos., 118, 11399-11418.

Fioletov, V.E. and McLinden, C.A. (2016). Sulfur dioxide (SO 2) vertical column density measurements by Pandora spectrometer over the Canadian oil sands. Atmos. Meas. Tech., 9, 2961.

Fioletov, V.E., McLinden, C.A., Krotkov, N., Li, C., Joiner, J., Theys, N., Carn, S. and Moran, M.D. (2016). A global catalogue of large SO 2 sources and emissions derived from the Ozone Monitoring Instrument. Atmos. Chem. Phys., 16, 11497.

Henney, L., Rodríguez, L. and Watson, I. (2012). A comparison of SO2 retrieval techniques using mini-UV spectrometers and ASTER imagery at Lascar volcano, Chile. B. Volcanol., 74, 589-594.

Jiang, J., Zha, Y., Gao, J. and Jiang, J. (2012). Monitoring of SO2 column concentration change over China from Aura OMI data. Int. J. Remote Sens., 33, 1934-1942.

JRC/PBL (2011). Emission Database for Global Atmospheric Research (EDGAR), release version 4.2. Retrieved June, 2017, from http://edgar.jrc.ec.europa.eu/.

Klimont, Z., Smith, S.J. and Cofala, J. (2013). The last decade of global anthropogenic sulfur dioxide: 2000–2011 emissions. Environ. Res. Lett., 8, 014003.

Krotkov, N., Carn, S., Krueger, A., Bhartia, P. and Yang, K. (2006). Band residual difference algorithm for retrieval of SO2 from the Aura Ozone Monitoring Instrument (OMI). IEEE Geosci. Remote S., 44, 1259–1266.

Krotkov, N., McLinden, C., Li, C., Lamsal, L., Celarier, E., Marchenko, S., Swartz, W., Bucsela, E., Joiner, J. and Duncan, B. (2015a). Aura OMI observations of regional SO 2 and NO 2 pollution changes from 2005 to 2014. Atmos. Chem. Phys., 15, 26555-26607.

Krotkov, N., Schoeberl, M., Morris, G., Carn, S. and Yang, K. (2010). Dispersion and lifetime of the SO2 cloud from the August 2008 Kasatochi eruption. J. Geophys. Res. Atmos., 115, D00L20.

Krotkov, N.A., Li, C. and Leonard, P. (2015b). OMI/Aura Sulfur Dioxide (SO2) Total Column L3 1 day Best Pixel in 0.25 degree x 0.25 degree V3, in: Greenbelt, M., USA, Goddard Earth Sciences Data and Information Services Center (GES DISC). Retrieved June, 2017, from http://giovanni.gsfc.nasa.gov/.

LEELŐSSY, Á., MOLNÁR, F., IZSÁK, F., HAVASI, Á., LAGZI, I. and MÉSZÁROS, R. (2014). Dispersion modeling of air pollutants in the atmosphere: a review. Open Geosci., 6**,** 257-278.

Lu, Z., Streets, D.G., de Foy, B. and Krotkov, N.A. (2013). Ozone Monitoring Instrument observations of interannual increases in SO2 emissions from

Indian coal-fired power plants during 2005–2012. Environ. Sci. Technol., 47, 13993-14000.

Nikolić, D., Milošević, N., Mihajlović, I., Živković, Ž., Tasić, V., Kovačević, R. and Petrović, N. (2010). Multi-criteria analysis of air pollution with SO2 and PM10 in urban area around the copper smelter in Bor, Serbia. Water Air Soil Poll., 206, 369-383.

OPEC. (2017). Annual Report 2017. OPECNA. & Information Dept., Vienna, Austria. Retrieved August, 2018, from https://www.opec.org/opec_web/static_files_project/media/downloads/publications/AR%202017.pdf.

OPEC. (2013). Annual Report 2013. OPECNA. & Information Dept., Vienna, Austria. Retrieved August, 2018, from https://www.opec.org/opec_web/static_files_project/media/downloads/publications/AR_2013.pdf.

OPEC. (2009). Annual Report 2009. OPECNA. & Information Dept., Vienna, Austria. Retrieved August, 2018, from https://www.opec.org/opec_web/static_files_project/media/downloads/publications/AR2009.pdf.

OPEC. (2005). Annual Report 2005. OPECNA. & Information Dept., Vienna, Austria. Retrieved August, 2018, from https://www.opec.org/opec_web/static_files_project/media/downloads/publications/AR2005.pdf.

Parkinson, C., Ward, A., King, M. (2006). Earth science reference handbook: a guide to NASA's earth science program and earth observing satellite missions.

Salmabadi, H. and Saeedi, M. (2018). Determination of the transport routes of and the areas potentially affected by $SO_2$ emanating from Khatoonabad Copper Smelter (KCS), Kerman province, Iran using HYSPLIT. Atmos. Pollut. Res., doi: 10.1016/j.apr.2018.08.008.

Smith, S.J., Aardenne, J.v., Klimont, Z., Andres, R.J., Volke, A. and Delgado Arias, S. (2011). Anthropogenic sulfur dioxide emissions: 1850–2005. Atmos. Chem. Phys., 11, 1101-1116.

S.P.G.C. (2018). Introduction of South Pars Gas Complex. Retrieved August, 2018, from http://www.spgc.ir/en/.

Theys, N., Campion, R., Clarisse, L., van Gent, J., Dils, B., Corradini, S., Merucci, L., Coheur, P., Van Roozendael, M. and Hurtmans, D. (2013). Volcanic SO2 fluxes derived from satellite data: a survey using OMI, GOME-2, IASI and MODIS. Atmos. Chem. Phys., 13, 5945-5968

Wang, J., Park, S., Zeng, J., Ge, C., Yang, K., Carn, S., Krotkov, N. and Omar, A. (2013). Modeling of 2008 Kasatochi volcanic sulfate direct radiative forcing: assimilation of OMI SO2 plume height data and comparison with MODIS and CALIOP observations. Atmos. Chem. Phys., 13, 1895-1912.